Numerical study on the flow in balancing hole

IOP Conf. Series: Earth and Environmental Science **240** (2019) 022002 doi:10.1088/1755-1315/240/2/022002

Numerical study on the flow in balancing hole

Jun Matsui, Atsushi Okubo, and Yousuke Yamashita

Yokohama National University, Tokiwadai 79-5, Hodogaya-ku, Yokhama, Japan
E-mail: jmat@ynu.ac.jp

Abstract. In order to investigate the value of discharge coefficient of balancing hole C_d for wide range of axial flow velocity v in the hole and rotational speed u, series of CFD simulations are made. Some of the result agrees well with the existing experimental data, but the difference is about 20% in some cases with high Re_v. Also, for wide area of Re_v, the effect of rotating speed u becomes significant. So it is considered that the parameter v/u is a dominant indicator of C_d. Furthermore, for very low range of v/u, we found a rare flow situation with S-shaped streamlines. In this flow, pumping of disk is so strong and Cd may differ largely.

1. Introduction

The value of discharge coefficient C_d in the balancing hole on Francis turbines or centrifugal pumps is very important to estimate both leak flow rate and axial thrust. This coefficient is already studied well by a lot of reports such as Wilk et al. [1], and it is usually expressed as a function of its shape and axial Reynolds number Re_v. The reported relations between the discharge coefficient C_d and Re_v are shown in Figure 1. Here the diameter of the balancing hole is defined as d, cross section of the hole is $A = \pi(d/2)^2$, pressure difference between inlet and outlet of hole is Δp, and the density of working fluid is ρ, volumetric flow rate in a hole is q, and the discharge coefficient is defined as

$$C_d \equiv \frac{q}{A\sqrt{\frac{2\Delta p}{\rho}}}.$$

Also a Reynolds number is defined as $Re_v=vd/(\mu/\rho)$, where the viscosity of working fluid is defined as μ, and average axial velocity in the hole is $v=q/A$, Besides, another Reynolds number using rotating velocity u is defined as $Re_u = ud/(\mu/\rho)$, where the radius of center of the hole is r_h, and angular velocity of runner or impeller is ω, and $u = r_h\,\omega$. The plots in Figure 1 have various inlet geometry of the hole, such as roundness of the corner.

In Figure 1, we show a model equation [3] as a solid line based mainly on Saito's data [2]. This model equation is defined as

$$C_d = \min(1.0,\ 0.00155 Re_v^{0.568}). \qquad (1)$$

Though this model equation is widely used such as in S008 standard, the reason of $C_d = 1$ for the area of $Re_v > 90000$ is not clear, and also estimated value at large Re_v does not agree with the result of Shimura et al. [4]. Additionally there remains a range of Re_v in which there is no experimental data, as you can see in the Figure 1.

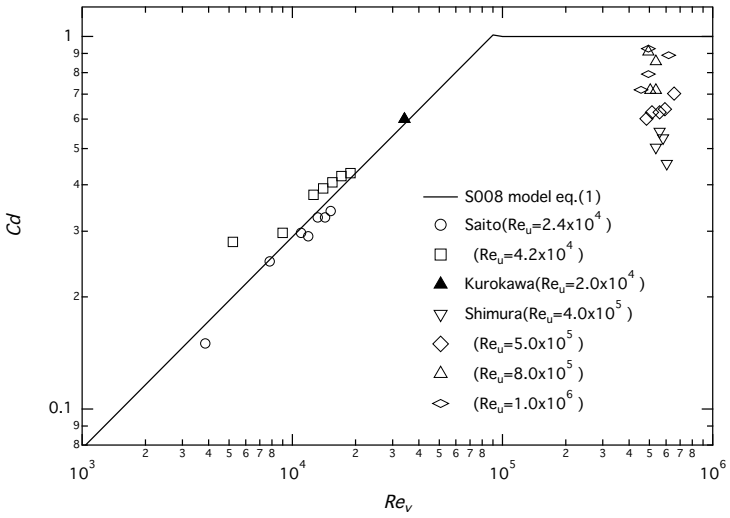

Figure 1. Relation between discharge coefficients of balancing hole and axial flow Reynolds number.

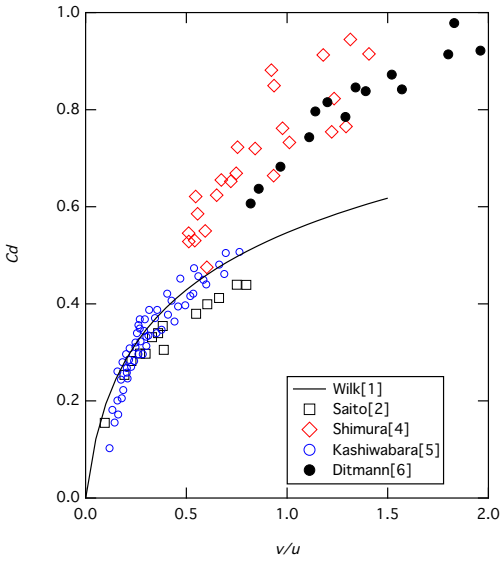

Figure 2. Relation between C_d and velocity ratio v/u.

On the other hand, Shimura et al. suggest that v/u, the ratio of axial flow velocity v and rotational velocity u, is a good parameter for C_d. This suggestion means that not only the Re_v but the Re_u has an effect to C_d. In Figure 2, the relation between C_d and v/u is shown. Though there are dissipation in the graph, the tendency of C_d is well reproduced by this parameter v/u. The solid line in Figure 2 is a model equation proposed by Wilk [1]. This equation is $C_d = 0.183 \ln((3/S) +1)$, where $S=u/(2\pi v)$. This also shows that the ratio of v/u is the dominant parameter for C_d.

Additionally, the discharge coefficient varies by the length of hole, fillet length, chamfer length, and so on [5,6]. So not only v/u but such parameters should be considered.

The use of CFD on the flow in balancing hole is studied by Karaskiewicz [7] for example, which shows the flow pattern and effect of vortex in the hole and so on. However, the range of Re_u is limited.

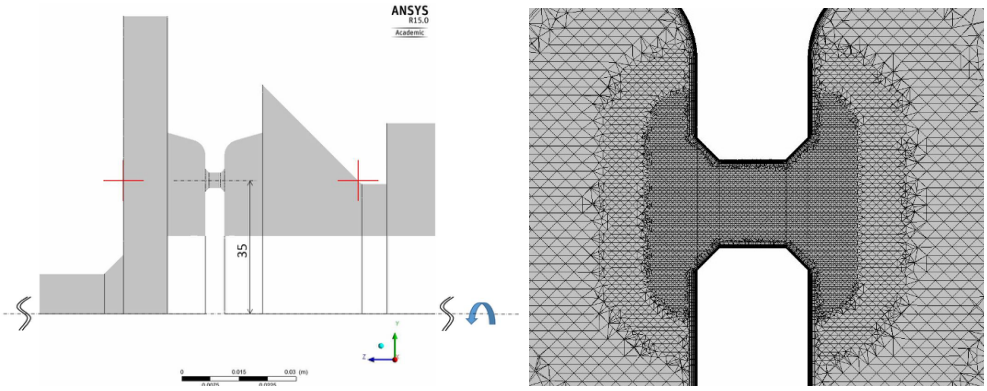

(a) Region of calculation (b) Grid lines near balancing hole

Figure 3. CFD area and mesh to reproduce experiments of Shimuras' [4].

Table 1. Analysis conditions.

Analysis Type	Steady Simulation
Turbulence Model	SST
Fluid	Liquid Nitrogen (77.2K, 1 atm)
Density	806.79 [kg/m3]
Viscosity	161.65 [Pa s]
Inlet Boundary Condition	Mass Flow Rate
Outlet Boundary Condition	Opening Pressure (1 [atm], abs.) and Flow Direction (Normal to Boundary)

Here we simulate flows in a balancing hole and calculate the discharge coefficients. After confirming the CFD results by comparing the result with some experiments, we calculate at some situations on which there is no experimental data with high Re_v or high Re_u value. In this process, we find that there are 2 types of flow patterns with dynamic change of C_d.

2. CFD results (1) comparison with Shimuras' experiment

The Shimuras' experiment [4] is a rare data for the high Re_v and Re_u. Here we simulate his experimental system in CFD using Ansys-CFX. Figure 3(a) shows the area of simulation. At the inlet, the mass flow rate is set as boundary condition. At the outlet the open boundary with a stationary pressure is used. Four pairs of mass flow rate and rotational speed are selected from the experiment. The analysis condition is shown in Table 1. The working fluid is liquid nitrogen (1[atm], 77.2[K]). Even when we change density and viscosity for 4[MPa] of nitrogen, the result was almost same.

The calculating mesh is a tetrahedron-type with 30 layers of prism-type, whose number of total node is about 1,250,000 and number of total element is about 4,220,000. The maximum y^+ is about 5.0 in all simulations, in which a blend between wall functions and low-Re formulations are used for small y^+ in CFX. Grid lines near balancing hole are shown in Figure 3(b).

The analysis condition and result are shown in Table 2. The maximum difference of C_d from experiment is about 30%, so present CFD should be modified more.

When we use the hexahedron-type mesh whose number of total node is 5,467,280 for calculation of case 4, the value of C_d becomes 0.623 and the difference is reduced to about 20.4%. Though we try to expand the calculating area and also try to change the pressure sampling positions which was not defined clearly in the report, we could not reduce the difference more than this.

Above simulations were made as steady calculations. As we show in next section the flow in the balancing hole has strong unsteadiness in some case, so we should try the unsteady simulation in the

near future. Also, in the experiment the flow rate is calculated ignoring the leakage at the seal on the outer edge of rotating disk. This leakage should be simulated, too.

The comparison between Shimuras' results and present CFD are shown in Figure 4. Though there is dispersion in this data, the tendency of C_d is well reproduced by present CFD.

Table 2. CFD conditions and results.

case	n[rpm]	(ρq) [kg/s]	v/u	C_d (Exp.)	C_d (CFD)	C_d Difference (%)
1	5180	0.270680	1.410	0.830	0.911	6.74
2	7073	0.256921	0.978	0.814	0.740	9.86
3	10761	0.288317	0.721	0.759	0.648	17.1
4	13666	0.275183	0.542	0.671	0.518	29.6

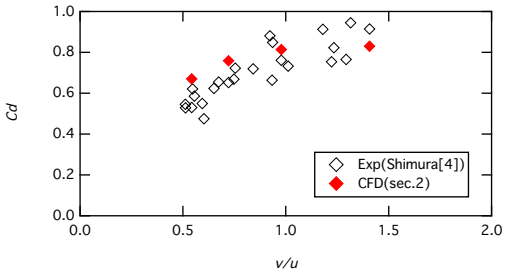

Figure 4. Comparison between CFD and Shimuras' experiment [4] and CFD.

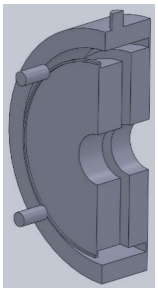

Figure 5. Total shape of experimental test section.

3. CFD results (2) comparison with Kashiwabaras' experiment

Next we try to reproduce Kashiwabaras' experiment [5]. As the disk has 6 balancing holes in this experiment, only the 1/6 of disk is calculated using periodical boundary condition along the tangential direction of disk.

The shape of experimental system is shown in Figure 5. The gray colored area is the fluid space. An example of calculating mesh is shown in Figure 6. In these calculations, hexahedron-type mesh is used. The center of Figure 6(a) is the balancing hole. The water as a working fluid comes from the left-top side in Figure 6(a). It goes through the hole to the container at right side of figure, then flow out from the right-top of the figure.

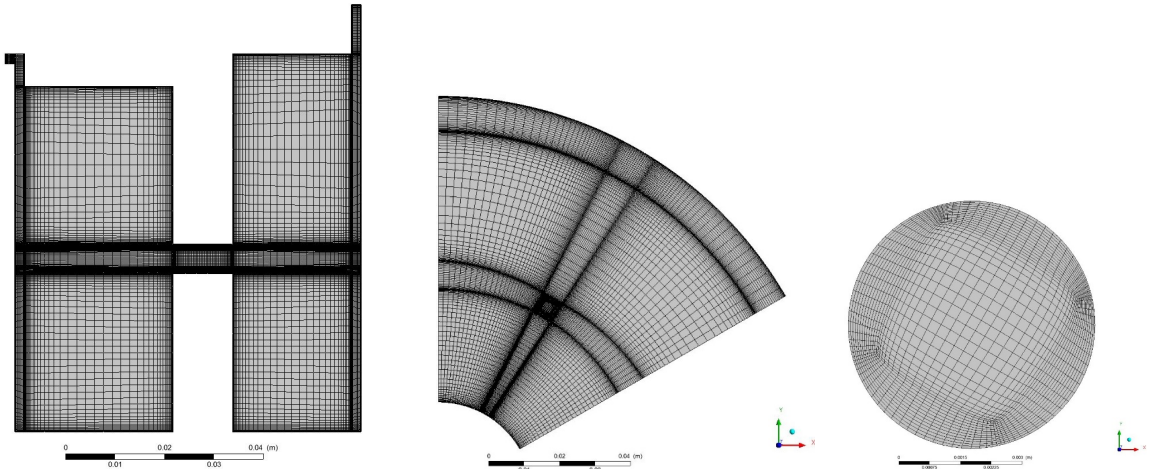

(a) cross section including rotating axis (b)cross section normal to rotating axis (c)cross section of balancing hole

Figure 6. Example of mesh for Kashiwabaras' cases.

Boundary conditions and turbulent model are same as them in previous section. In the steady calculation at flow rate q=2[L/min] and rotational speed n=1350[rpm], the residual continues to vary largely and we cannot get steady result. In the unsteady calculation, the velocity and pressure at the outlet of hole starts to vibrate periodically. However, the averaged Δp value in the unsteady simulation is almost same as that of steady simulation.

On the other hand, at different rotational speed n=930[rpm] with the same flow rate q=2[L/min], we can get steady flow by both steady and unsteady simulation. Therefore, we use unsteady simulation for all cases below.

The result at n=1350[rpm] almost agrees with the experiment result, with difference about 5.3%. Also difference at n=930[rpm] was 3.4%. We can get reliable CFD results with present mesh.

An example of velocity vector at n=1350[rpm] is shown in Figure 7. This figure is on a cross section which includes the axis of hole and parallel to the rotating axis. We are viewing this section from outer side of radius, and the arrows in the figure means the relative velocity to disk. The disk rotates from upper to lower in the figure, so the relative velocity near disk goes from lower to upper.

We can see a large vortex or separated area in the hole. The flow along the boundary layer in the left side of disk goes into the hole and flows near upper wall of hole, and flow out from the edge of hole. The stream from hole vibrates periodically. This causes the periodical vibration for Δp.

4. Flow field at high Re_v area

As we can get the reliable CFD result at the same condition of experiments, we try a lot of CFDs at the higher range of Re_v. For each calculating condition, we check that the mesh resolution is enough, using some meshes whose resolution is different.

Present results of CFDs of section 2 and 3 are shown in Figure 8, with reported experimental results. Though almost all CFD results uses the same shape without fillet or chamfer, the result varies widely.

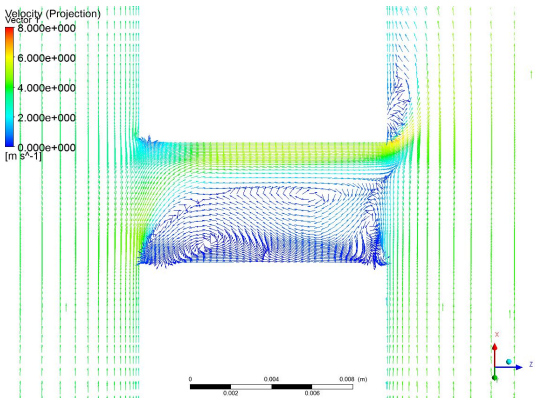

Figure 7. Velocity vector at n=1350[rpm].

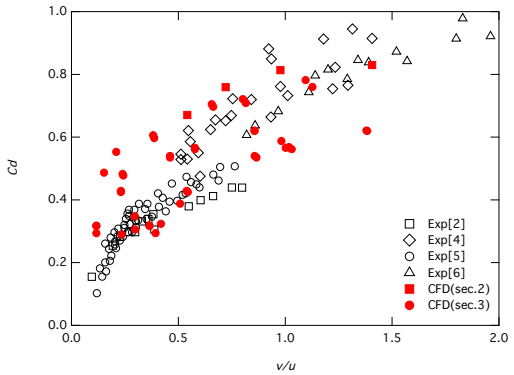

Figure 8. Cd Comparison between CFD and Experiments.

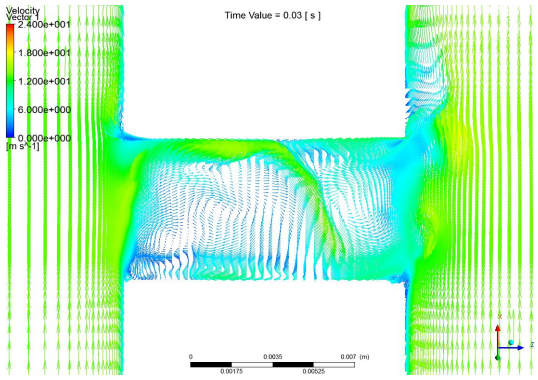

Figure 9. Velocity vector at n=4000[rpm].

By the way, we find a curious phenomenon that the flow field is suddenly changed at a rotating speed during the flow rate q is kept same value.

An example of velocity vectors after the sudden change at n= 4000[rpm] and q=2[L/min] is shown in Figure 9. The leakage flow in the hole flows with S-shape streamlines. This S-shape flow has strong unsteadiness.

At this situation, the Δp becomes very small, or in some cases the pressure at the outlet is larger than that at inlet of balancing hole. The relation between Δp and rotational speed is shown in Figure 10. In this case the flow field is suddenly changed near n=3000[rpm].

The pressure distributions along the axis of balancing hole with different rotational speeds are compared in Figure 11. This is an example at a time and it is not the time-averaged value. Thought the pressure at the outside of hole is almost same, it varied largely in the hole ($0.45< Z/Zh < 0.62$). As the

rotational speed is increased, the pressure in the upstream area at $Z/Zh < 0.45$ is reduced. Because in this simulation the pressure at downstream boundary is fixed, the change of Δp can be seen at the upstream side. At n=4000 and 5000[rpm]case, the stationary pressure becomes larger during the flow goes through the hole. This increase of pressure is a result of acceleration of flow in the hole by the rotation of disk, that is a kind of pumping effect by the disk.

As equation 1, the flow in the balancing hole was modelled as a passive pipe with some loss, but these CFD results indicate that we must consider the effect of pumping from the disk. This effect should be estimated quantitively in the future.

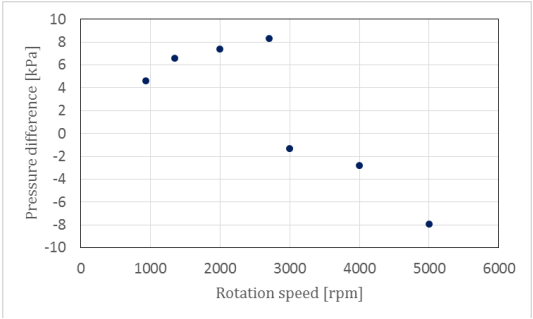

Figure 10. Pressure difference at hole at q=2[L/min].

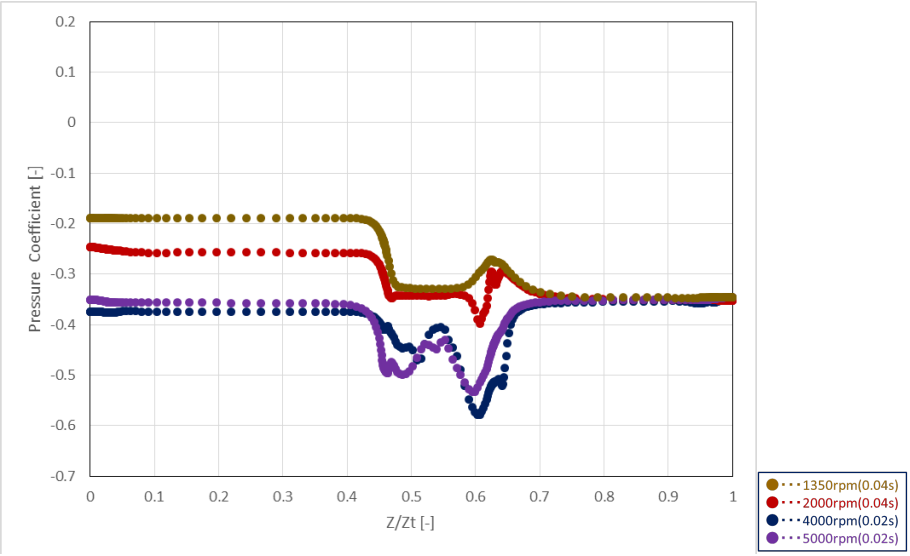

Figure 11. Pressure distribution on hole axis.

We can see the above phenomenon in every CFD trial such as modifying the mesh from hexahedron to tetrahedron type, changing number of mesh, adding a small chamfer at both inlet and outlet edge of hole, changing the limit of convergence, changing the turbulent model from SST to LES. Thus, this phenomenon is considered as not virtual but actual, and should be confirmed by experiments in the future.

To understand these flow patterns, let's consider the q=0 case for example. In this situation, on the cross section of Figure 9 two vortexes will occur by the relative fast flow near the surface of rotating disk, as shown in Figure 12(a). When a small amount of leak flow is added to this situation, the leakage may be transported by these vortexes as shown in Figure 12(b). This may be the case in the figure 9. When the q becomes large, as Figure 12(c), the leakage flow may enhance one vortex and make the other vortex disappear, as in the Figure 7.

Therefore, a S-shaped flow with curious Δp may occur only when the rotational speed n or u is large against the leakage flow rate q or v, that is, only when v/u is very small. Because q becomes large when n is large usually, the flow pattern as Figure 12(b) may be rare in the practical turbo machinery.

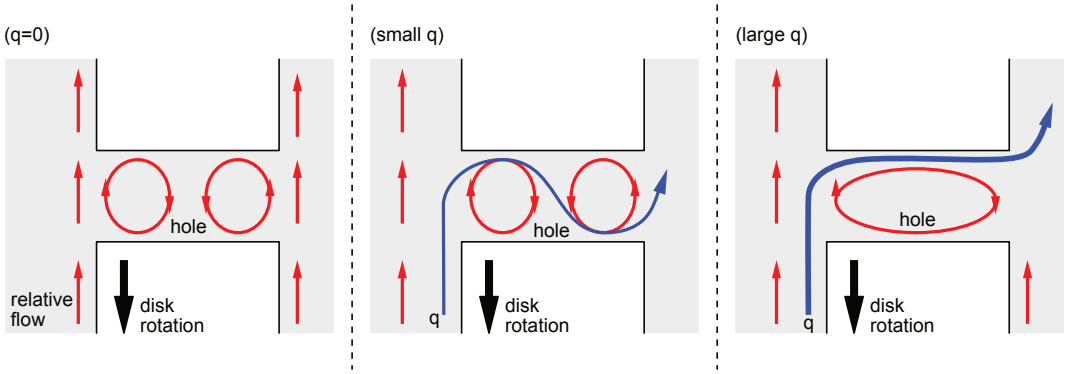

Figure 12. Model flow patterns according to the leakage flow rate.

5. Conclusion

The flow in the balancing hole is analyzed by CFD simulation under same condition of some experiments and also under expanded conditions. From the results, below conclusions are brought.

- Though some difference of discharge coefficient exist, CFD result agrees with the experimental ones.
- The parameter v/u or Rev/Reu is a dominant parameter of Cd, considering the effect of rotational speed u.
- When v/u is very small, the pumping effect becomes large, and the flow in the hole becomes to S-shape pattern. This phenomenon should be verified by some experiments in the future.

References

[1] Wilk A 2015 *Experimental Thermal and Fluid Science* **54** 297
[2] Saito S 1978 *Turbomachinery* **6** 330 (in Japanese)
[3] Kurokawa J 1990 *Bulletin of JSME* B **56** 185 (in Japanese)
[4] Shimura T and Hasegawa T 1993 *Japan Society for Aeronautical and Space Sciences*, **41** 590 (in Japanese)
[5] Kashiwabara T and Toyokura T 1993 *Turbomachinery* **21** 300 (in Japanese)
[6] Dittmann M, Dullenkopf K and Witting S 2004 *Journal of Engineering for Gas Turbines and Power* **126** 803
[7] Karaskiewicz K and Zloty L 2015 *Transactions of The Institute of Fluid-Flow Machinery* **130** 57